Chapter

Study of Non-predictive Patterns of Non-Ionizing Radiation in the City of Salta in Argentine

Mario Marcelo Figueroa de la Cruz and Roberto Daniel Breslin

Abstract

Non-ionizing radiation (NIR) is a subject of continuous debate despite having been regulated internationally and at the level of organizations in all countries. This debate is focused on the level of population exposure to non-ionizing radiation density, since there is no certain evidence of the level of safety of the values adopted ranging from 0.2 mW/cm^2 to 0.2 uW/cm^2 according to the regulations of each state. The radiation precisions are made with models that evolve to take into account most of the factors that can attenuate the radiation emitted from an antenna from free space to models that take reflection and diffraction as attenuation factors. However, our work deepens in a phenomenon that is verified in measurement campaigns that is one of the values that do not fit with predictive models and that, on the contrary instead of showing attenuation, have higher values than expected. This work shows the results of observation campaigns of these points and their relationship with environmental conditions, which present diverse probabilities to explain their condition.

Keywords: non-ionizing radiation, population exposure, antennas, cellular telephony

1. Introduction

1.1 The characteristics of a normal radiation

A normal non-ionizing radiation (NIR) is that which is produced from a radiation mechanism based on electromagnetic propagation and its propagation components; that is, it follows a radiation mechanism where the electromagnetic wave encounters a discontinuity in its path waveguide, being forced to change the shape of longitudinal propagation within a closed environment to a spread radiation in an open environment.

The typical discontinuity that is used for the radiation to be efficient and allows controlling to some degree the propagation of an essentially isotropic radiation and transforming it into a directional radiation is the element called antenna.

An antenna, in essence, transforms an ideal isotropic radiation into a radiation that concentrates, in a certain direction, in the energy coming from a source of

electromagnetic radiation. In this chapter, we analyze the characteristics of the normal radiations that generate predictive patterns based on the propagation characteristics and those of the antennas with respect to non-predictive patterns. To verify this alteration of the patterns, measurement points with discordant values were obtained in a specific campaign.

2. Elements of radiation

2.1 The antenna and its gain

The energy radiated by an antenna will be distributed uniformly in all directions and with divergent direction of the source, which in this case is the antenna, this case is also ideal since the radiation cannot be precise considering that the antenna does not it is more than a discontinuous prolongation of a transmission line and therefore has a feature of balanced line or balanced lines, this implies the existence of two elements or arms and therefore an antenna is basically a dipole.

This implies that, in essence, the radiation will have zero in the directions axial to the axis of that dipole.

In this way, if the dipole is placed with alignment to the Z axis, that is to say in a vertical position, the radiation null will be at ±90 of the dipole antenna itself.

In the case that the antenna is aligned with the axis y or x, the minimum radiation will be aligned with the corresponding axis.

However, the generality for broadcasting or cell phone transmission dipole antennas has an orientation on the Z axis in such a way that the main polarization is the so-called vertical polarization.

This means that the electric field vector has the same direction as the originating antenna, i.e., vertical (aligned with the Z axis), and that the magnetic field vector is of horizontal orientation since it will always be perpendicular to the vector of magnetic field enunciated in Maxwell's equations.

Radiation emitted by a dipole is conditioned by two factors that are not directly related to propagation or radiation and if the electrical characteristics of the circuit between a transmitting device and an antenna are:

- Adaptation efficiency
- Radiation efficiency

The adaptation efficiency depends on the adaptation of impedances between the transmission line and the antenna, where what is sought is that the impedance of the antenna constitutes the conjugate transpose of the impedance of the transmission line in which case the adaptation is perfect (**Figure 1**).

$$R_r + R_\Omega = R_g \tag{1}$$

$$X_A = -X_g \tag{2}$$

The radiation efficiency is specified by the relation between the totality of the energy that is delivered by the transmission line to the antenna and the energy actually radiated by it. The ideal situation is for the antenna to behave as an

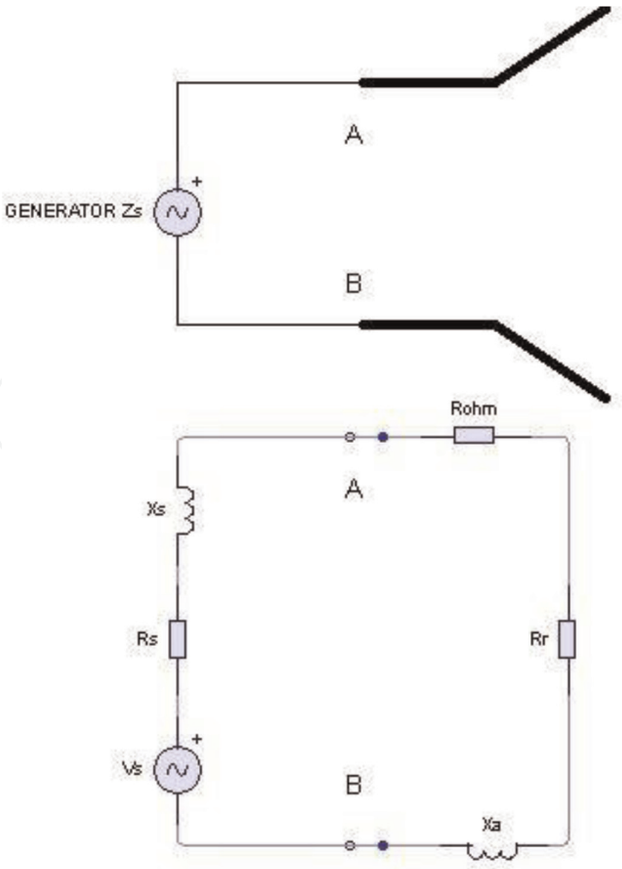

Figure 1.
Thevenin model of transmission of an antenna.

electrical element of resistance equal to zero, so that 100% of the energy delivered is radiated, this being an unrealizable situation; however, a part of the energy delivered is transformed into heat by Joule effect and is conditioned by the quality of the physical components of the antenna.

Therefore, the gain is conditioned by two efficiencies in such a way that the gain must be affected by the relationship between the impedance of the line and the antenna and the relationship between the ohmic and radiation resistances.

$$\eta_r = \frac{R_r}{R_r + R_\Omega} \tag{3}$$

$$Ca_T = \frac{P_A}{P_{AMAX}} = 1 - |\rho|^2 = 1 - \left|\frac{ROE - 1}{ROE + 1}\right|^2 \tag{4}$$

$$\rho = \frac{Z_L - Z_O}{Z_L + Z_O} \tag{5}$$

However, these considerations are not the only ones to be carried out for wireless communication and in particular for cellular telephony due to two factors:

- Limitation on profit
- Unequal coverage

2.2 The limitation of profit

The gain of an antenna is defined based on a factor called directivity.

The directivity is a factor that is given by the deformation of the radiation lobe that has a dipolar antenna and is measured as a relationship between a totally isotropic radiation and the radiation of a lobe that has an angular aperture bounded by a certain value less than that of isotropic radiation that has a 360-degree lobe.

The directivity can be defined as the lobe whose opening is limited by the angles that limit radiation with a drop of 3 decibels with respect to the maximum.

So the lobe will have a maximum of radiation in some direction and will have a smaller amount of radiation in directions with different angles from the maximum, that angle where it is verified that falls 3 decibels with respect to the maximum constitutes the limit of the radiation lobe or half power points. In short, the angle of opening will be twice the angle between the direction of the main lobe and the direction of the points of half power.

Obviously, the energy is not dispersed but is concentrated within the radiation lobe, i.e., the Poynting vector of the radiation lobe will have its maximum in the main direction of it and will decrease in different directions to that of the main lobe (**Figure 2**).

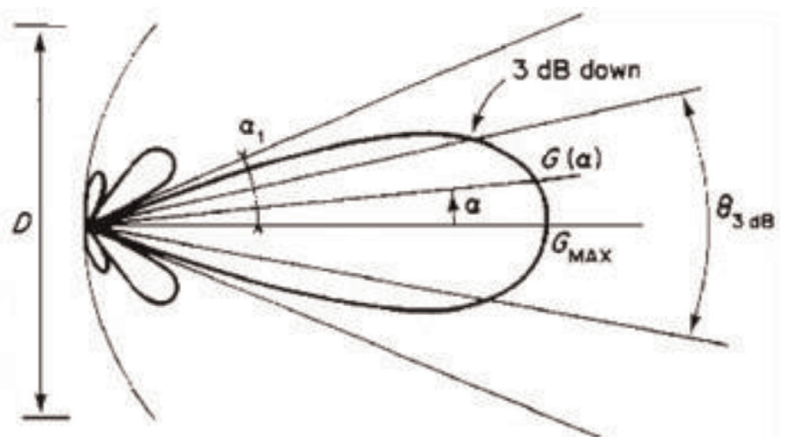

Figure 2.
Directivity of an antenna.

The gain of the antenna as previously expressed depends directly on the directivity so that the lower the opening of the lobe, the greater the verified directivity and, consequently, the greater the gain allocated to the antenna.

As a consequence, the Poynting vector has a much higher value in the main direction of the radiation lobe, where the greater part of the radiated energy is concentrated, so that to have greater radiated energy, a greater directivity is needed.

That is why what is sought in an antenna, in most cases, is the directivity, since having more energy in the center of the lobe, the attenuation will have a lesser effect and you can have a communication that arrives with good energy level at a greater distance.

The design of an antenna is based on the fundamental premise that the radiation lobe, both vertically and horizontally, is calculated for the electric field of the radiated wave.

However, the search in wireless communications is based on achieving the maximum use of radiated energy to achieve propagation distances as long as possible, which are why the gain of the antenna is the main factor in the efficiency of telecommunications.

2.3 Uneven coverage

Coverage is the geographical area in which the energy radiated by a radiator element such as an antenna has such a value that it can be exploited by an electronic receiving device.

That is, it is the area where the signal has a suitable value so that the receiving electronic equipment can adequately transform the electromagnetic signal into an electrical signal with an adequate signal-to-noise ratio in order to be intelligible information.

Depending on the type of coverage required, it will be the characteristic of the antenna that is used to radiate.

If what is required is an omnidirectional radiation, a dipole antenna is more than enough; however, it is precisely this antenna that has the lowest gain and, therefore, although it achieves an omnidirectional coverage, the attenuation it suffers is so strong that the coverage it has is very deficient.

That is why, for the omnidirectional coverage, antennas with a characteristic in the horizontal lobe of high aperture and in the vertical radiation lobe of high directivity are used.

A generic situation is to achieve the 360° coverage by antennas that have a horizontal lobe opening of 120° placing in this case three antennas or even placing 6 antennas with 60° openings.

As far as the coverage in distance is concerned, it depends on the vertical lobe opening and how it is required to achieve the widest possible coverage. It is required that the effects of the attenuation in the free space be compensated by the high gain or directivity that the antenna has.

For this, antenna panels with apertures smaller than 20° are used (**Figure 3**).

This coverage is usually referred to as the footprint of the antenna and the situation generates that in the areas closest to the antenna there is more radiation in the case that the center of the radiation lobe is aimed at the point closest to the antenna.

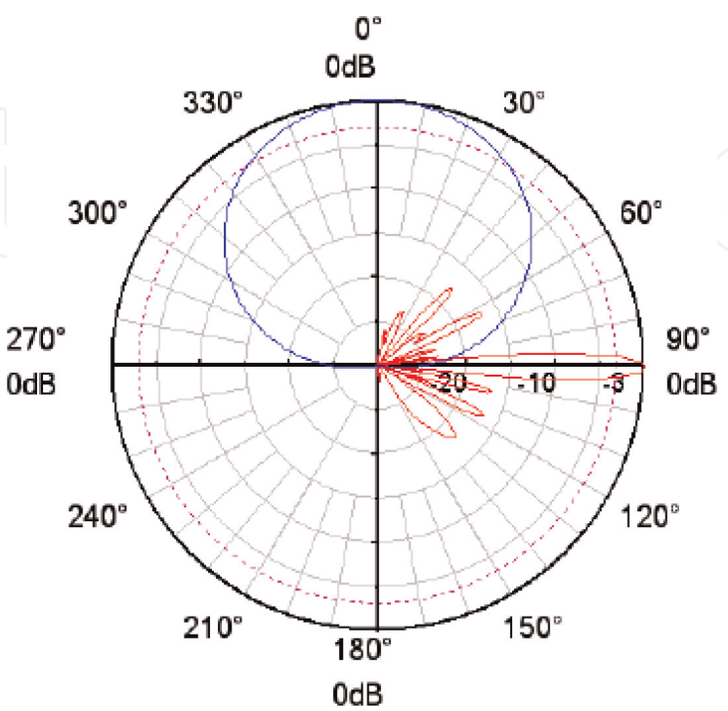

Figure 3.
Huawei Dual Band Panel Radiation Diagram ADU4518R3 [1].

What is required, for a good coverage, is that all users have reasonably the same level of signal. It is customary to make the center of the radiation lobe point toward the most extreme point, so that the signal level at the most extreme point coincides with the maximum of the radiation lobe. In the same way, those points that coincide with the minimum values of the radiation ovule, i.e., the 3 decibel points, are those that have less attenuation by distance.

In this way, the radiation lobe will tilt such that the level of radiation that will suffer the least attenuation by distance will fall at the point of coverage closest to the antenna and that the center of the radiation lobe having the highest power will suffer the greater attenuation in such a way that the coverage is equalized between both extremes and the users do not feel the decrease of the signal given by the attenuation in the free space (**Figure 4**).

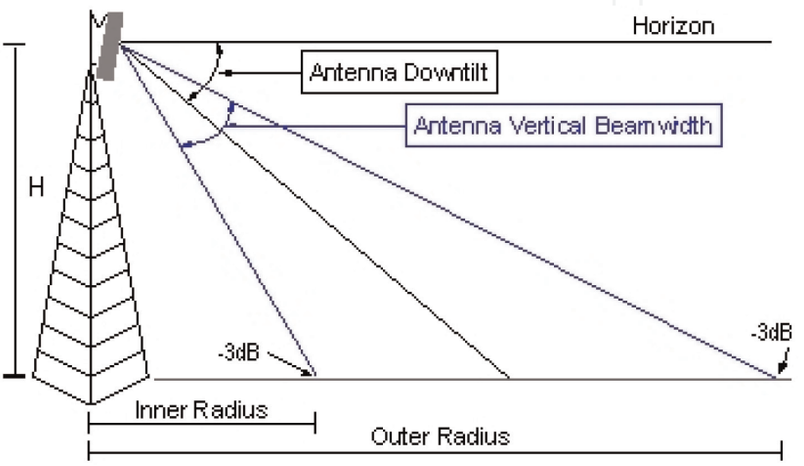

Figure 4.
Coverage method by downtilt [2].

It is evident that the height of the tower on which the antenna is located has a direct influence on the coverage area; however, there is a limitation that has to do with the attenuation in the free space so that the height of the tower has a practical limit that has to do with coverage and attenuation.

$$\text{Inner Radius Distance} = \frac{H/\text{Tan}\left(A + \frac{BW}{2}\right)}{5280} \tag{6}$$

$$\text{Outer Radius Distance} = \frac{H/\text{Tan}\left(A - \frac{BW}{2}\right)}{5280} \tag{7}$$

where A is the downtilt angle of the main beam, H is the height of the antenna relative to the ground, and BW is the angle of opening of the lobe for 3 dB of fall with respect to the main lobe.

These trigonometric equations give us the rule that the largest distance will depend on the angle of inclination that is the lowest, possibly and logically, and will also depend on the height of the tower as it has a direct proportionality.

It is very evident that if the value of the bandwidth of the beam width is 15° half of it will be 7° and the minimum distance of radiation from the base of the antenna would be corresponding to 7°. However, this would imply that it is directly pointing down. (A = 90°), which is not feasible or economically acceptable.

Considering that the Poynting vector analyzed practically how radiation density per unit area is 100 watts over square centimeters, a normal tread has a radiation

density value of the order of 0.2 W/cm^2. This value is very important to take into account in the study of electromagnetic emission, derived from the radiation of a cell phone installation, characterizing the emission in the exclusive values of the frequency spectrum used by this application, for which the considered emission is in the values of 700 megahertz at 2.3 GHz

These values are directly related to the tread and with the radiated power from the radio bases and correspond to an average value of −79 decibels.

Mobile cellular equipment in turn will change its data reception system depending on the signal level in such a way that when receiving a signal lower than this value, it will automatically change to Enhanced Data Rates for GSM Evolution (EDGE) or General Packet Radio Service (GPRS) mode.

Therefore, the signal level will directly affect the speed of the internal modems of cellular equipment.

2.4 The antennas

Another aspect that has to be taken into account is what is normal radiation has to do with the emitting antennas.

The mobile telephone antennas are characterized by being bi-directional (emission or reception) of low power. In addition to producing RF radiation, they are mounted on poles, transmission towers, or the roofs of tall buildings, since they need to be at a certain height in order to have a wider coverage.

In a typical mobile telephone antenna, the radio emission is made toward the front and horizontally, in the form of a substantially flat beam, and covers a sector between 60 and 120°. Emissions are almost non-existent in the other directions (back, bottom, and top).

The characteristics of the antennas and the conditions in which they are usually installed make the emission levels in terms of radiation density very low in the place where they are located.

The flat panel antennas, as the name suggests, are a square- or rectangular-shaped panel. And they are configured in a patch-type format. Flat panel antennas are very directional since most of their radiated power is a single direction in either the horizontal or the vertical plane. In the elevation pattern (**Figure 5**) and in the azimuth pattern (**Figure 6**) [3], you can see the directivity of the flat panel antenna.

The flat panel antennas can be manufactured in different directivity values according to their construction. This can provide excellent directivity and considerable gain.

These panels, in fact, are an array of 4 or 5 antennas whose separation between each other within the panel and the different paths that run through the signal in the waveguides that feed them provide an additional tilt (called an electric tilt).

The angle of inclination of the main lobe is the sum of the mechanical TILT (conditioned by mobile supports) and the electric TILT given by the regulation of the paths (phase delays) of the power supply of each antenna of the array installed in a panel (**Figure 7**).

2.5 Calculation of normal radiation

Normal radiation follows a predictive pattern in which there are components that allow to know what is the power density value in the surface based on:

- The power with which the antenna is fed
- The attenuations of the connections

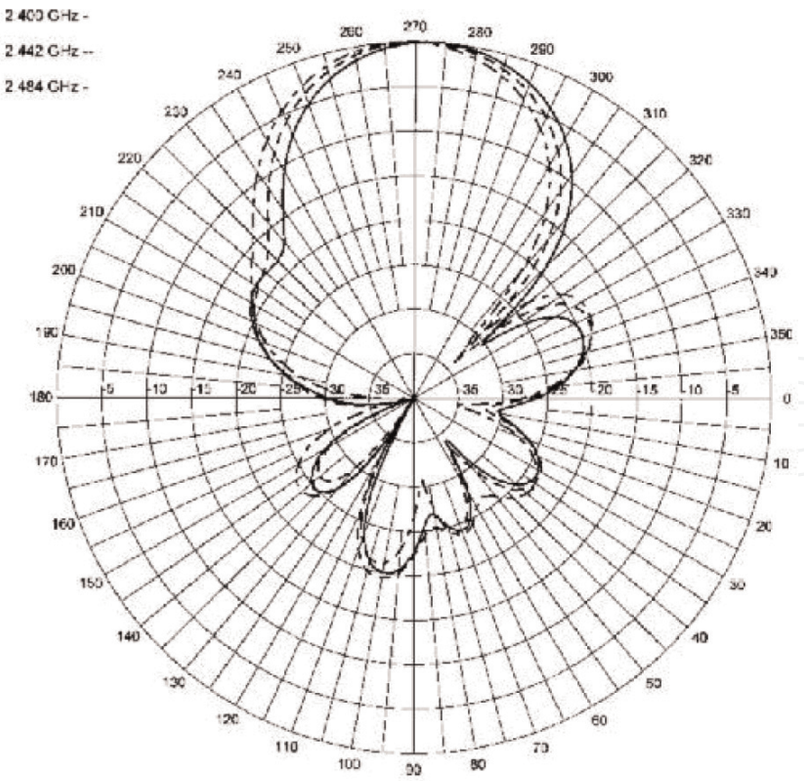

Figure 5.
Flat elevation pattern high gain panel [3].

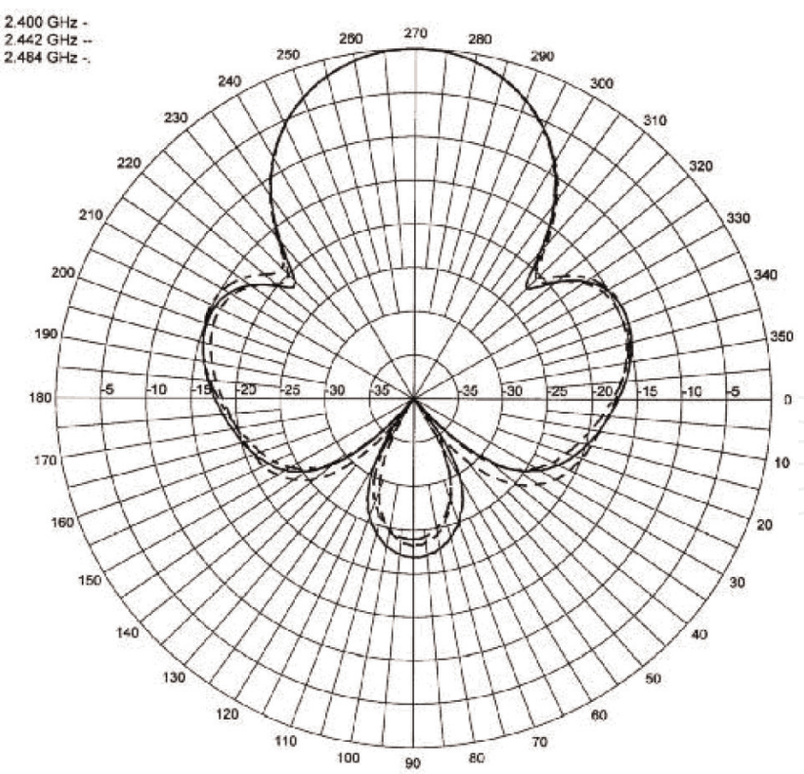

Figure 6.
Azimuth flat high gain panel pattern [3].

- The antenna gain affected by the coupling coefficients and radiation loss coefficient
- The attenuation in free space

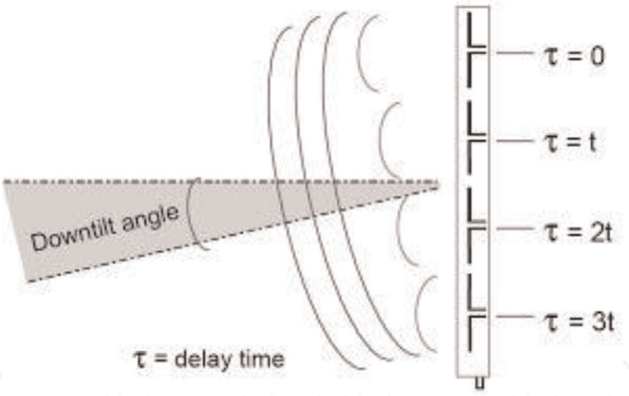

Figure 7.
Angle of an array of antennas caused by different phases [4].

The resulting value can still be added to a variety of attenuations produced by the surrounding environment that can be characterized as:

- High density urban
- Urban low density
- Suburban
- Rural

These attenuation parameters have been contemplated in various models such as the following:

2.5.1 Propagation model in free space

This model is used to predict the power of the signal when there is a clear line of sight between the transmitter and the receiver. Satellite communication systems and microwave links can be modeled as free space propagation. The free space model predicts that the received power decays as a function of the separation distance between the transmitter and receiver raised to some power. The power received in the free space by a receiving antenna, which is separated from the transmitting antenna by a distance d, is given by the equation.

$$Pr\,(d) = PtGtGr\,\lambda 2/(4\,\pi)2\,d2\,L \tag{8}$$

Where Pt is the transmitted power, Pr is the received power that is a function of the Tx-Rx separation (transmitter-receiver), Gt is the transmit antenna gain, Gr is the gain of the receiving antenna, D is the separation distance of Tx-Rx given in meters, λ is the wavelength given in meters, and L depends on the obstacles, line of sight is = 1.

The equation shows that the power of the received signal is attenuated to form the square of the distance between the transmitter and the receiver, which implies that 20 dB /decade decays.

2.5.2 Okumura model

The Okumura model [5] is one of the most widely used for signal prediction in urban areas. This model is applicable for frequencies in the range of 150–1920 MHz,

that is, it comprises the VHF and UHF band (however, it is typically extrapolated for frequencies above 3000 MHz entering the SHF band) and distances of 1 Km to 100 Km. It can be used for antenna heights of the base station in the range of 30–1000 m.

The model can be expressed as:

$$\text{L50 (dB)} = \text{LF} + \text{Amu (f, d)} - \text{G (hte)} - \text{G (hre)} - \text{GAREA} \tag{9}$$

where L50 (dB) is the median attenuation per trajectory, LF is the free space attenuation, Amu (f, d) is the average relative attenuation (curves), G (htx) is the height gain of the Tx antenna, G (hrx) is the height gain of the Rx antenna, and GAREA is the gain due to the type of environment.

Okumura found that G (hte) varies at an index of 20 dB/decade and G (hre) varies at an index of 10 dB/decade for heights less than 3 m.

G (hte) = 20log (hte/200) for 30 m < hte < 1000 m

G (hre) = 10log (hre/3) for hre < 3 m

G (hre) = 20log (hre/3) for 3 m < the <10 m

It is one of the simplest and most suitable models for attenuation predictions.

2.5.3 Hata model (Okumura-Hata)

It is an empirical formulation of the propagation loss data provided by Okumura and is valid in the frequency range of VHF and UHF, from 150 to 1500 MHz. Although Hata [5] presented the losses within an urban area as a standard formula:

$$\begin{aligned}\text{L50 (urban) (dB)} = {} & 69.55 + 26.16 \log \text{fc} - 13.82 \log \text{hte} - \text{a (hre)} \\ & + (44.9 - 6.55 \log \text{hte}) \log \text{d}\end{aligned} \tag{10}$$

Taking into account that:

150 MHz < fc <1500 MHz

30 m < hte <200 m

1 m < hre <10 m

It should be considered that the definitions are the same as for the Okumura model, including:

- fc: carrier frequency [MHz].
- the height of the transmitting antenna in [m] in the range from 30 to 200 meters.
- hre: receiving antenna height in [m] in the range from 1 to 10 meters.
- a (hre): correction factor for the effective height of the mobile antenna that is function of the type of service area.
- d: distance between transmitter and receiver [km].

As can be seen, it involves a new variable that is the correction factor of the mobile antenna and is defined according to the size of the city:

For small- and medium-sized cities:

$$\text{a (hre)} = (1.1 \log \text{fc} - 0.7)\,\text{hre} - (1.56 \log \text{fc} - 0.8)\,\text{dB} \tag{11}$$

For large cities:

$$a\,(hre) = 8.29\,(\log\,1.54hre)\,2 - 1.1\ \text{dB for fc} < 300\ \text{MHz} \tag{12}$$

$$a\,(hre) = 3.2\,(\log\,11.75hre)\,2 - 4.97\ \text{dB for fc} > 300\ \text{MHz} \tag{13}$$

The following is the formula that can be used in a suburban environment:

$$L\,(dB) = L50\,(urban) - 2\,[\log\,(fc/28)]\,2 - 5.4 \tag{14}$$

For rural areas:

$$L\,(dB) = L50\,(urban) - 4.78\,(\log\,fc)\,2 + 18.33\log\,fc - 40.94 \tag{15}$$

This model adapts very well for the design of large-scale systems, but not for PCS systems, which have cells of the order of 1 km radius. For this purpose, a numerical-empirical formulation of the graphical data provided by Okumura of attenuation for urban areas is made.

2.5.4 Model cost 231 (extension of the Hata model)

The European Cooperative for Scientific and Technical Research (EURO-COST) [5] developed the COST 231 model, in which it extends the Hata model up to the 2 GHz range covering the VHF and UHF bands. The model is expressed as:

$$\begin{aligned} L50\,(urban) = {} & 46.3 + 33.9\,\log\,fc - 13.82\,\log\,hte - a\,(hre) \\ & + (44.9 - 6.55\,\log\,hte)\,\log\,d + CM \end{aligned} \tag{16}$$

where CM is a correction factor to adapt the model by extending the frequency range for which the Hata model operates, CM is 0 dB for medium-sized cities and suburban areas, CM is 3 dB for metropolitan centers, and a (hre) corresponds to the equations presented in the previous topic (Hata Model).

One of the contributions of this model is to consider dispersion losses.

It is also defined in the following range:

f: 1500–2000 MHz

Th: 30–200 m

hre: 1–10 m

d: 1–20 km

2.5.5 Calculations based on normative resolution N° 3690/04

Although the above are mitigation calculations, the regulations applied in Argentina are those issued by CNC (National Communications Commission) under resolution number 3690 of 2004 [6].

In the aforementioned, reference is made to the fact that prior to any measurement, a predictive calculation based on attenuation in space must be made, which takes into account the antenna power to calculate the radiation density in relation to the distance.

$$S = \frac{\text{PRA}\ .1{,}64.2{,}56.\text{F}^2}{4.\pi.\text{r}^2} \tag{17}$$

where S is the power density in $\frac{W}{m^2}$, PRA is the antenna power in W, F is the attenuation at times of radiation at a certain angle of incidence in the vertical plane if it is unknown to adopt 1, 2.56 is an empirical reflection factor that takes into account the possibility that fields reflected in phase can be added to the direct incident field, and R is the distance from the antenna in meters.

3. Background on normal RNI measurements

Measurements of non-ionizing radiation are clearly developed not only with a number of works on the subject, only to exemplify the work of Azpurua et al. [7], the thesis work of Br. Jorge Juan Eduardo Ríos Solar [8], or the work that preceded it [9] and the relevant regulations in Argentina. In all these works and even regulations, measurements are made or measurements based on the theoretical radiation lobes are standardized of the installations taken as a reference for the emission of non-ionizing radiation.

3.1 Normal measurements made

This research developed a plan of field measurements, which focused on areas already studied in the project "Analysis of Measurements of Non-Ionizing Radiation in the City of Salta from the UCASAL" [9]. It was extended for 2 months in the areas studied and new areas.

The methodology emanating from RES N ° 3690/04 was used because the following stipulations were applied:

3.1.1 Selection criteria for measuring points

- The measurement must be made at accessible points by the public.
- The measurement points will be chosen according to the characteristics of the system.
- Irradiation and the wavelength of the emissions, where "applicable a the predictive calculations".
- For omnidirectional systems, at least 16 points should be selected, conveniently located on the ground, whose separation from the station is a function of the wavelength of the emitter.

Factors that influence the response of the instruments:
The following should be taken into account when making measurements:

- Variation of the impedance of antennas or probes in the vicinity of conductive surfaces
- Capacitive coupling between the probe and the field radiation source

The influence of these factors can be reduced by maintaining a separation greater than 20 cm or three times the size of the probe, whichever is greater, with respect to the source of re-irradiation field. That is why it is recommended that the antennas and/or probes are installed on tripods of non-conductive material.

3.1.2 Instruments used

In all cases, the instruments used were a TES-92 and TM-190 (TENMARS); previously, a contrast of measurements was made with an NARDA −550 that was taken as a calibration standard in a total of 25 measurements, the dispersion of results of 10% for TES-92 and 22% for TM-190, so the measurements presented correspond (unless specific indication) to TES-92.

The characteristics of the instrument are:

- Sensor type: electric field (E)
- Frequency range: 50–3.5 GHz
- Directional characteristic: isotropic, three-dimensional
- Measuring range (signal >50 MHz): 20 mV/m up to 108.0 V/m
- Error of use (@ 1 V/m and 50 MHz): ± 1.0 dB
- Frequency response (taking into account the number Factor CAL Factor: ±1.0 dB (50 MHz–1.9 GHz), ±2.4 dB (1.9–35 GHz)
- The noise deviation: Type. ±1.0 dB f > 50 MHz
- Load limit: 4.2 W/m^2 (40 V/m)

3.1.3 Normal measurement site Miguel Ortiz

The Miguel Ortiz site is an area centered on a monopost and located in the northern area of the city of Salta. It is characterized for being a suburban and quasi-rural location, since two of the panels partially cover areas corresponding to the field. It also covers an area of the Bolivian avenue that is an urban continuation of the highway of the same name. That is why in the path marked according to the regulations, there are rough areas of absolute clearance and line of sight (**Figures 8** and **9**).

Some deviations (attributed to motorway conditions) can be seen, although the trend of the curve follows a predictive pattern

3.1.4 Normal measurement site Castañares

This site is relevant because the first 150 ms of separation from the antenna are in free space due to the presence of a clear field; here, the installation is of a self-supporting tower 40 meters high (**Figures 10** and **11**).

3.1.4.1. Linear correction factor

A correction by footprint is made linearly from the point of −3 dB not taking into account the real lobe but an approximation that does not take secondary lobes into account.

$$K = 0.707 + (1 - 0.707)/(198 - 108).(\text{Distance} - 108) \qquad (18)$$

Figure 8.
Miguel Ortiz site measurement area.

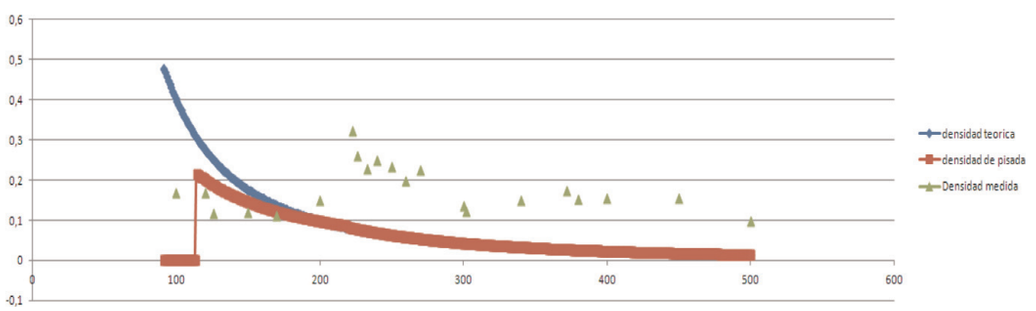

Figure 9.
Graph of radiation density measurements and predictive patterns. Miguel ortiz site.

Figure 10.
Castañares site measurement route.

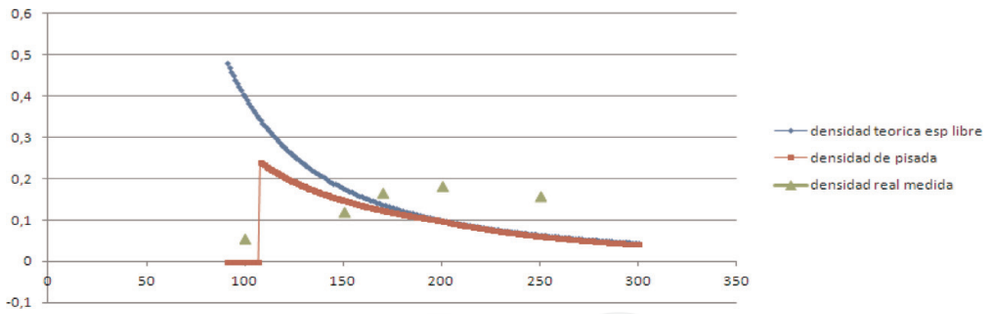

Figure 11.
Graph of radiation density measurements and predictive patterns. Castañares site.

3.1.5 Conclusions of normal measurements

In both cases, it can be observed that there is a clearance at least in the first section of the measurement and that it responds to the calculation trend taking into account the theoretical tread.

The uniformity in density values along the tread is also denoted, which is a desirable effect and compatible with an expected behavior for mobile telephony coverage.

4. Non-predictive patterns

During the measurement process referred to in the work "Analysis of Measurements of Non-Ionizing Radiation in the City of Salta from the UCASAL" [10], a series of random measurements were taken and also values were found that do not respond to a predictive pattern within urban trajectories and in trajectories in suburban environments but with sufficient clearance to be considered with little incidence of buildings; however, it was observed that there are phenomena that cannot be predicted with the stated models since they correspond to the attenuation in the free space and this is added in all cases of additional attenuations.

The cases that are listed show sites where, in the level of radiation density, not only does it not follow a predictive pattern, but also the level of radiation density increases.

4.1 History of discordant measurements

4.1.1 Aeroclub Salta site

The measurement in the Aeroclub Salta site constitutes the first measurement parameter discordant with the applied theory from the point of view of both the attenuation in the free space and the correction by tread (**Figures 12** and **13**).

The point located at 200 meters and the point located at 180 meters completely change the predictivity of the measurement; although the scope of measurement is free space in most of the path, the jarring factor is given in a point close to metal signage with a minimum height of 3 meters.

4.1.2 Guayacanes Site

This is a completely suburban site in the Tres Cerritos neighborhood of the City of Salta. It is a self-supporting tower 65 meters high and has a large number of panels as it is used by three telephone companies to provide service in the area.

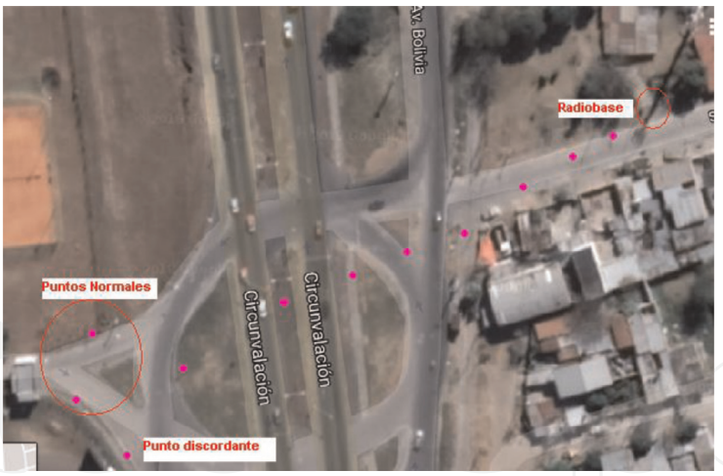

Figure 12.
Measurement trajectory and discordant points. Aeroclub Salta site.

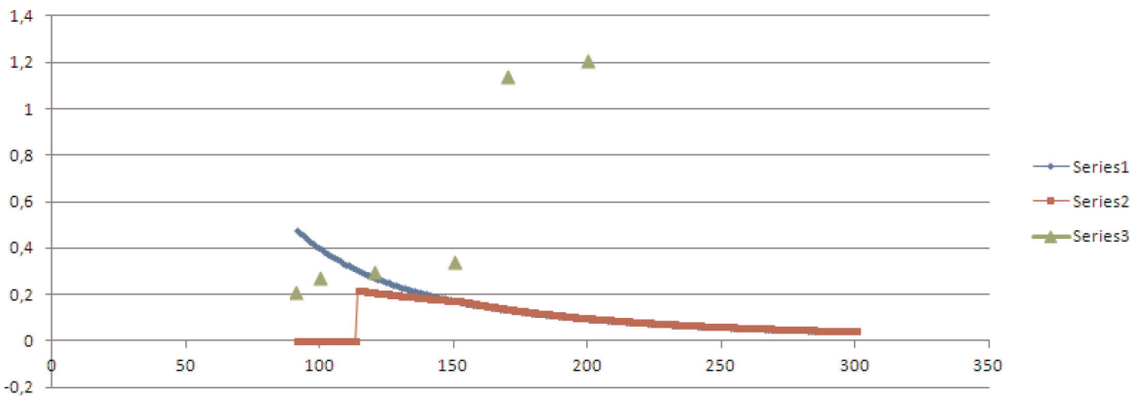

Figure 13.
Graph of radiation density measurements and predictive patterns. Aeroclub Salta site.

Measurements followed a path in a street (Las Acacias) that provides a line of sight of good quality and there is even a square with ample clearance (**Figures 14** and **15**).

The values measured in this area are much higher than the trend, and additionally, they are punctual since, as the advance of the planned measurement path continues, they return to their normal value.

It can be seen that in a high clearance area there are highly discordant points

Figure 14.
Measurement trajectory and discordant points. Guayacanes site.

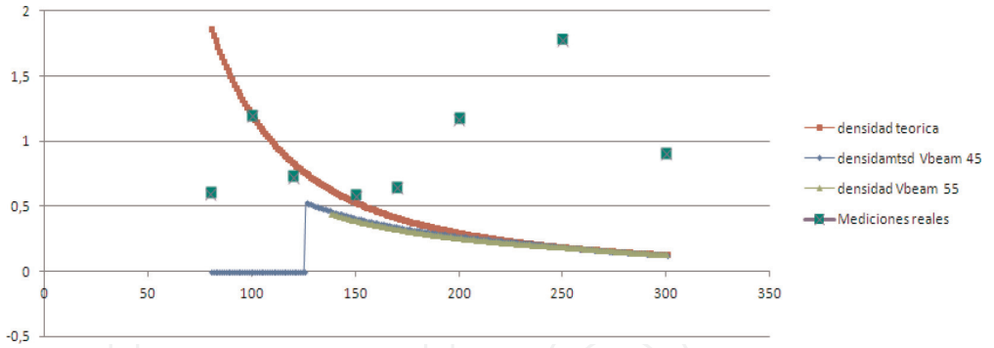

Figure 15.
Graph of radiation density measurements and predictive patterns. Guayacanes site.

4.1.3 Considerations regarding low-frequency radiation

The aerial lines of low- and medium-voltage lines are in some cases considered as causing a probability of increase in the radiation density by radiofrequency, which is why it is worth considering what the applicable concept of immission is and what the ranges of measurement of the immission sensors used by the instruments are.

4.1.3.1 Definition of Immission

As can be inferred from [11], "this term refers (in law) to an attack, aggression or attack of environmental type or also to a concentration, agglutination or conglomeration of pollution or the transfer of pollutants in a place or site and at a specific moment, more in common in the air and in general to an electromagnetic energy or radioactive particles."

The analysis of the definition is very useful because the agglutination does not imply a sum necessarily (it is an essentially biological concept) [12] and the possibility of a concentration.

In the case of electromagnetic immission, it must be considered that the sensors used for measurement are made in the three electric field vectors (x and z) and the sum is a vector sum of these fields.

However, the sensed fields start from frequencies from 100 Khz. If we consider the harmonic spectrum of an electrical network, this would correspond to a harmonic of order 2000, considering 50 Hz as fundamental frequency, so it cannot be considered to the radiation of electric lines as a member of the emission that can be measured by RNI sensors.

Such is the case that there are no sensors with such a large bandwidth to detect RF radiation with values below 100 KHz [13], and in fact the detectors are based on Schottky diodes with bounded bandwidths, hence the need to change the probe for certain high-frequency measurements.

5. Measurements of points that do not respond to predictive patterns

5.1 Work methodology

In the research project "Analysis of non-predictive patterns of non-ionizing radiation in a sector of the northern area of the City of Salta" approved by the

research council of the UCASAL a plan of measurements inside and outside lobe trajectories is planned of radiation, a work methodology and a measurement protocol were implemented in accordance with the objective of identifying and characterizing points where the radiation value exceeds the normal value of the area. Off-trajectory measurements were also made from radiation lobes centered on radio bases with the sole purpose of verifying the possible existence of other points of discordance, not with a radiation pattern but with their close environment.

Thus, random routes were generated with a permanent measurement methodology with configurable alarm instrument, and it was particularized in density levels higher than 1 uW/cm^2.

For the field measurements, both the TES-92 meter (which exclusively measures the emission in a range of 300 KHz–2.5 GHz) and the TM-190 meter that measures a range of 50 MHz–3.5 GHz of RNI were used. And additionally, it measures electromagnetic and electric field radiation separately in the frequency of 50 to 60 exclusively. The objective of this double measurement was to contrast the presence of abnormal values of electric fields in conditions of electromagnetic fields relevant to this study.

5.2 Background of "hot" points

In informal measurements prior to the launch of the measurement campaign, 4 points were found where the level greatly exceeds the level of 1 uW/cm^2, reaching values of 2.75 uW/cm^2. That measurement campaign was launched with the aim of finding other points and analyzing the environmental conditions in order to establish a prediction pattern.

5.3 Work hypothesis

5.3.1 Metallic surfaces

As a consequence of the aforementioned antecedents, the possibility arises that there are specific locations, or small areas where phenomena of increase in the level of radiation density are manifested that are not a consequence of the emission produced by antenna radiation, but of other factors which are related to the environment of the point in question.

There is sufficient evidence of the increase in light radiation at infrared frequencies and visible by the effects of the surfaces on which they affect, such as the case of Raman scattering. [14] When light interacts with matter, it can disperse inelastically from vibrational quantum states. During this process, the photons can lose energy, or gain it from vibratory excitations, and it can also produce a concomitant change in the scattered frequency. The phenomenon, called the Raman effect, was discovered experimentally in 1928 by C. V. Raman and K. S. Krishnan in India and, independently, by Leonid Mandelstam and Grigory Landsberg in the former Soviet Union.

Oldenburg SJ, Hale GD, Jackson JB, and Halas NJ postulate in their work Light scattering from dipole and quadrupole nanoshell antennas [15] that metal nanoshells are nanoscale optical components that allow the controllable redirection of electromagnetic radiation through a careful engineering of its multilayer structures. By varying the size of the core and the thickness of the shell of these nanoparticles, nanoscale "antennas" are constructed that can be selectively driven in a dipolar or quadrupole oscillation pattern. With spaced transverse sections many times larger than their physical cross-section, these antennas are efficiently coupled

to the incident electromagnetic wave. These structures can focus, redirect, or divide incident light

In this sense, Martin Moskovits in his work Surface-Enhanced Spectroscopy [16] reveals that molecules adsorbed on specially prepared silver surfaces produce a Raman spectrum that is sometimes a million times more intense than expected. This effect was called improved surface Raman scattering (SERS). Since then, the effect has been demonstrated with many molecules and with several metals, including Cu, Ag, Au, Li, Na, K, In, Pt, and Rh.

Another factor that could be the cause of non-predictive patterns is stated in the work of Francisco J. Rodríguez-Fortuño, Giuseppe Marino, Pavel Ginzburg, Daniel O'Connor, Alejandro Martínez, and Gregory A. W, Near-Field Interference for the Unidirectional Excitation of Electromagnetic Guided Modes [17], where they postulate that wave interference is a fundamental manifestation of the superposition principle with numerous applications. Although in conventional optics, the interference between waves that experience different phase advances during propagation, the vector structure of the near field of an emitter is essential to control its radiation, since it interferes with the interaction with a mediating object. Then, the near-field interference of a circularly polarized dipole results in the unidirectional excitation of the electromagnetic modes guided in the near field, without a preferred far-field radiation direction.

With these studies, it can be postulated that in the vicinity of certain surfaces there may be abnormal concentrations of radiation with respect to a prediction based on the propagation models from a source based on an antenna and that there is a dependence of the characteristics of this abnormality with the polarization that occurs in the near field of the source, so not all antennas could produce constructive interferences.

Under this hypothesis is that a campaign of measurements focused on the probability of finding hot spots of radiation density in certain environmental conditions, in particular, metallic reflective surfaces or with reflective paints, is required.

It is a possibility that these points are the consequence of antennas or panels that have circular polarization characteristics, that is, discarding the linear polarization dipoles.

5.3.2 Electric distribution transformers

Although the emission should not be related to power lines, it is no less true that the process of transforming voltage with high power levels could generate harmonics that contribute to the emission, whose value could be a significant analysis of the presence of transformers in the vicinity of points of high radiation density.

5.3.3 Buildings of 2 or 3 floors that could produce reflections

Resolution ITU No P526-11 is a methodology that includes a series of predictive patterns taking into account a variety of effects of buildings on the radiation pattern by diffraction [18] and most other propagation models also take into account reflection effects. It is necessary to identify the presence of buildings with a differential height with respect to the normal level of buildings; in this sense, it will take into account only the buildings very close to the points of differential radiation of electromagnetic density.

For these purposes, a non-predictive non-ionizing radiation measurements protocol was designed.

6. Protocol of measurement of RNI under non-predictive patterns

In order to systematize the analysis of the environmental conditions that could eventually generate points with differential RNI levels, a working protocol was established based on the hypothesis that certain elements or constructive characteristics could be generating the points with radiation differentials with respect to normal radiation in the area.

6.1 Measurement protocol of non-predictive patterns

1. A known radiation source of omnidirectional radiation must be determined in the UHF or higher bands whose radiation model is omnidirectional. To this end, the application Cell Network Info lite or similar should be used in an Android phone to locate the antenna on which the route will be based.

2. An analysis grid will be drawn identifying the route to be carried out. For this purpose, radial routes to the location of the tower should be prioritized.

3. A walking tour will be started by holding the TES 92 meter or similar in a hand at an approximate height of 1.60 meters above ground level, your own cell phone or any other device that can emit radiation (e.g., Bluetooth) must be deactivated.

4. The field analyst must observe the radiation indicator At all times looking for radiation patterns that exceed the normal nominal values of the area by 100% or more.

5. Upon the detection of a value such as stated above, proceed as follows:

   a. The field analyst will stop or start a scan in the detailed area looking for the point where the maximum radiation is detected.

   b. At that point, he will proceed to do the following:

      i. Record the exact coordinates of the site.

      ii. Photograph the meter at that point.

      iii. Take the meter to a nearby point where the radiation level is significantly lower.

      iv. Record the coordinates of this point.

      v. Photograph the meter in the foreground and in the background the place where the significant level was verified.

      vi. Return to the point where the significance was verified.

   c. He will make an observation of the physical/constructive characteristics of the place, emphasizing the following aspects:

      i. Constructions or parts of metal buildings both solid and grilled.

      ii. Metal signage nearby.

      iii. Surfaces that can be identified as reflective.

      iv. Metal gates.

v. Vehicles parked in the vicinity (in this case, check again when the vehicle is not).

vi. Painted surfaces with some type of metallic or shiny paint.

vii. Presence of obvious radiation sources (such as antennas, transformers, welding machines, electric motors in operation, generators, etc.).

viii. Any other aspect of the environment that is relevant.

d. He will photograph the surrounding environment and place particular focus on the constructions or elements listed.

6. Continue the journey under the rules stated.

7. Results of measurements under protocol of measurement of RNI under non-predictive patterns

Table 1 shows the values found taking into account the value of the point found and the value of its environment, obtaining the differential value. The table is ordered in descending order with respect to the differential.

7.1 Analysis of sites with non-predictive values of radiation level

From the analysis of **Table 1**, the following conclusions can be obtained:

- The radius of a point of high differential radiation is variable and does not depend on the center's RNI level.

- The radiation differential between the maximum and the normal level is not directly related to the maximum level of radiation.

- The observed average radius is 1.81 mts.

7.2 Analysis of the relationship between points of high level of radiation and distance to the most likely site of emission

Table 2 is shown in order to determine the possible relationship between the proximity to the emission source and the points with the highest differential value of radiation density with respect to the normal values of the site.

7.2.1 Conclusions of analysis of the relationship between points of high level of radiation and distance to the most likely site of emission

From **Table 2** and **Figure 16**, it can be seen that there is no relationship between the increase in the differential of radiation and the distance to the most probable source of radiation since, for example, for a distance to the site of most likely emission of 100 meters, radiation differential values as different as 16.95 uW/cm^2 $\frac{uW}{cm^2}$ are appreciated as 0.81 uW/cm^2.

ID site	Coordinates	Dif real-normal	Level l $\frac{uW}{cm^2}$	Normal level $\frac{uW}{cm^2}$	Radius (mts)
9-Rioja 880	−24.76664, −65.39294	16.95	20.15	3.2	0.5 a 1
14-Avda. Independencia 1286	−24.80827, −65.39923	16.14	17.64	1.5	4
8-Rioja 862	−24.77988, −65.40314	7.71	8.51	0.8	0.4 a 0.9
12-Avda. Paraguay y J Castellanos	−24.80575, −65.4197	4.134	5.058	0.924	2
15-Avda. Independencia 1290	−24.80828, −65.39889	4.05	5.25	1.2	3
7-Rioja 842	−24.7813, −65.40111	2.859	3.599	0.74	0.9 a 1.5
4-Florida y San Luis	−24.77664, −65.40431	2.772	4.011	1.239	0.4 a 1
5-Florida 602	−24.7796, −65.40132	2.609	3.223	0.614	0.3 a 07
Avda. Uruguay 735	−24.7813, −65.40111	2.026	3	0.537	4
20-Mendoza “Lago del Parque”	−24.79541, −65.4028	1.602	3.152	1.55	2
16-Avda. Independencia 1326	−24.80825, −65.39829	1.26	2.06	0.8	2
Avda. del Bicentenario 800	−24.77988, −65.40314	1.19	2	0.33	5
25-Sarmiento y 12 de Octubre	−24.77378, −65.41483	1.161	1.791	0.63	1
18-Santa Fe y Mendoza	−24.79534, −65.4045	1.138	1.738	0.6	2
2-Santa Esq. Rioja	−24.76743, −65.39803	1.067	2.533	1.466	0.5 a 1
19-Mendoza 2	−24.79551, −65.40302	0.935	1.735	0.8	3
Avda. Uruguay 895	−24.7796, −65.40132	0.9	1	0.253	1
23-Aniceto Latorre y A. Güemes	−24.77307, −65.41625	0.883	1.57	0.687	1
22-San Martin Y Lavalle	−24.79374, −65.40344	0.85	1.45	0.6	3
26-Sarmiento y 12 de Octubre	−24.77416, −65.41455	0.811	1.261	0.45	2
Vicente López 1000	−24.77664, −65.40431	0.81	1	0.22	4
24-Aniceto Latorre y A. Güemes	−24.77309, −65.41596	0.719	1.029	0.31	1
11-Lamadrid y Lola mora	−24.80426, −65.42133	0.7	1.3	0.6	1
Los Jazmines 840	−24.76403, −65.3905	0.667	0.777	0.11	3

ID site	Coordinates	Dif real-normal	Level l $\frac{uW}{cm^2}$	Normal level $\frac{uW}{cm^2}$	Radius (mts)
Avda. Uruguay 751	−24.78087, −65.4012	0.663	0.955	0.292	2
Vicente López 1075	−24.77694, −65.40427	0.621	0.934	0.313	2
6-Rioja 710	−24.78087, −65.4012	0.601	1.141	0.54	0.5 a 1
Los Jazmines y Los Mandarinos	−24.76664, −65.39294	0.587	0.6	0.013	10
21-Mendoza "Paseo"	−24.79544, −65.40224	0.511	1.523	1.012	2
1-Santa Fe 698	−24.76403, −65.3905	0.421	1.071	0.65	1 a 1.5
13-Avda. Independencia y calle Pucha	−24.80825, −65.40466	0.4	0.7	0.3	1
17-Avda. Independencia 1360	−24.80827, −65.39797	0.3	0.5	0.2	2
Av. Reyes Católicos 1617	−24.76743, −65.39803	0.294	0.535	0.241	1
3-Rioja Esq. Catamarca	−24.77694, −65.40427	0.21	0.89	0.68	0.3 a 0.7
Los Ombúes 95	−24.76449, −65.39652	0.129	0.226	0.097	3
10-Jujuy 804	−24.76449, −65.39652	0.06	0.61	0.55	0.4 a 0.8

Table 1.
Results of samples under non-predictive pattern measurement protocol.

7.3 Analysis of the incidence of the proximity of transformers of electrical distribution with respect to the differential of radiation density

7.3.1 Conclusions of the analysis of the incidence of the proximity of transformers of electrical distribution with respect to the differential of radiation density

From **Table 3** and **Figure 17**, it can be concluded that the presence of electrical distribution transformers does not constitute a conditioning factor for the point increase in the level of differential radiation density. However, the lack of influence in the specific increase cannot be guaranteed since they have an incidence of 27% in the total of events.

7.4 Analysis of the incidence of the proximity of billboards, gates, or metal fences with respect to the differential of radiation density

7.4.1 Analysis of the incidence of the proximity of signage, gates, or metal fences with respect to the differential of radiation density

According to working hypothesis 4.3, the analysis of metal surfaces near points of high differential level of radiation density is of particular interest.

Real-normal dif of S in $\frac{uW}{cm^2}$ x 100	Theoretical radiation source (mts)
1695	100
1614	15
771	80
413.4	200
405	20
285.9	70
277.2	200
260.9	100
202.6	38
160.2	250
126	30
119	86
116.1	245
113.8	200
106.7	70
93.5	220
90	194
88.3	370
85	400
81.1	200
81	94
71.9	360
70	3
66.7	400
66.3	63
62.1	90
60.1	150
58.7	400
51.1	250
42.1	50
40	300
30	50
29.4	300
21	50
12.9	420
6	300

Table 2.
Differential radiation density values as a function of distance to probable source.

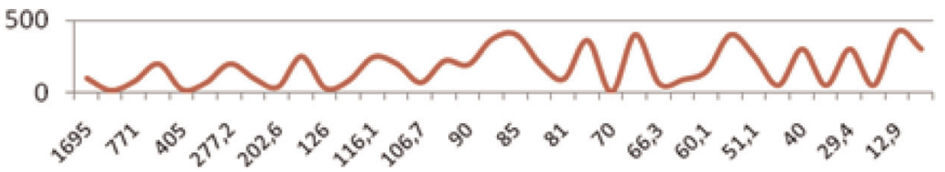

Figure 16.
Differential radiation density as a function of distance to probable source.

From **Table 4**, the following can be concluded:

- Some surface 89%
- Metal posters 27%
- Metal gates 57%
- Fences 68%

The probability increases by 30% if there is more than one metal surface in the vicinity (**Figure 18**).

Having some type of metallic surface, there is an 89% chance of finding a point with radiation density differential (**Figure 19**).

7.5 Analysis of the relationship between nearby buildings and the radiation level differential

7.5.1 Analysis of the relationship between nearby buildings and the radiation level differential

From **Table 5**, the following can be concluded:

- Some building 84%
- Buildings of 2 floors 73%
- Buildings of 3 floors or more 22%

In 84% of the cases of differential increase in radiation density, there is a building with 2 or more floors nearby, although the presence of these two types of buildings only increases the possibility by 0.06%.

7.6 Other factors analyzed

The following additional factors have been taken into account as a probable factor of point increase:

- Influence of vegetation and trees
- Pavement
- Metallic ceilings
- Electrical wiring
- High density of parked vehicles

Real-normal differential $\frac{uW}{cm^2}$	Proximity of transformers (mts)
16.95	1
16.14	0
7.71	1
4.134	0
4.05	0
2.859	1
2.772	0
2.609	0
2.026	0
1.602	0
1.26	1
1.19	1
1.161	0
1.138	0
1.067	0
0.935	0
0.9	0
0.883	0
0.85	0
0.811	0
0.81	0
0.719	0
0.7	1
0.667	0
0.663	0
0.621	0
0.601	0
0.587	0
0.511	0
0.421	0
0.4	0
0.3	1
0.294	0
0.21	1
0.129	1
0.06	1

Table 3.
Presence of distribution transformers in relation to differential level of radiation density.

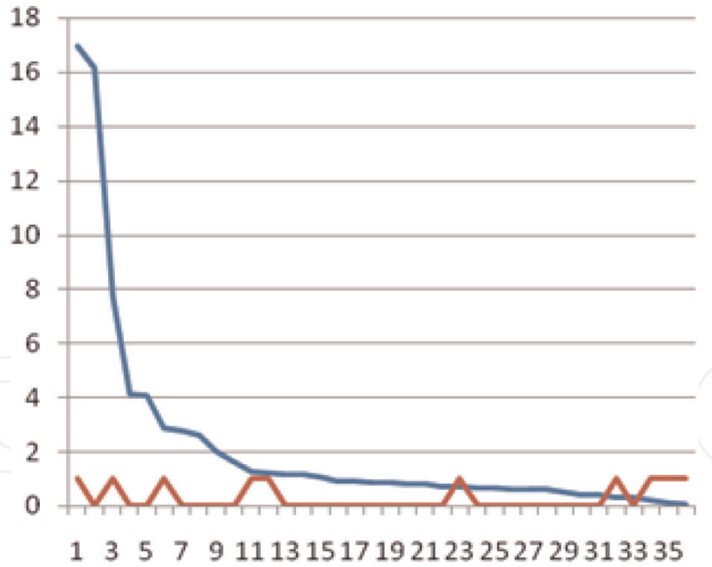

Figure 17.
Cases of presence of distribution transformers in relation to differential level of radiation density (y axis).

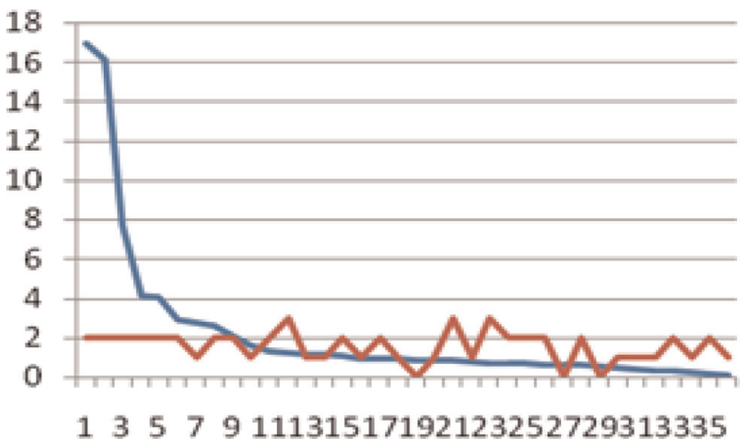

Figure 18.
Incidence of the number of cases of metallic surfaces with respect to the differential of radiation density.

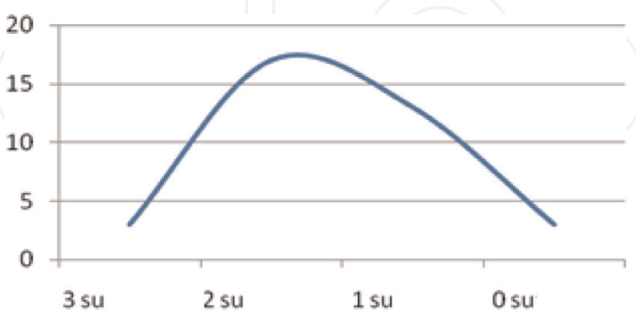

Figure 19.
Distribution of probability of increase of differential level of radiation density according to the amount of metal surfaces nearby.

7.6.1 Analysis of the influence of other factors on the differential and on the point value of radiation density

In this analysis, it is possible to deepen the point radiation according to its value. From the analysis of **Table 6**, the following can be concluded:

Differential real-normal $\frac{uW}{cm^2}$	High metal signage cases	Metal gates cases	Metal fences/wiring cases	Number of cases
16.95	0	1	1	2
16.14	0	1	1	2
7.71	0	1	1	2
4.134	1	0	1	2
4.05	0	1	1	2
2.859	0	1	1	2
2.772	0	0	1	1
2.609	0	1	1	2
2.026	0	1	1	2
1.602	0	0	1	1
1.26	1	1	0	2
1.19	1	1	1	3
1.161	0	0	1	1
1.138	1	0	0	1
1.067	1	1	0	2
0.935	0	0	1	1
0.9	1	1	0	2
0.883	0	0	1	1
0.85	0	0	0	0
0.811	0	0	1	1
0.81	1	1	1	3
0.719	0	0	1	1
0.7	1	1	1	3
0.667	0	1	1	2
0.663	0	1	1	2
0.621	0	1	1	2
0.601	0	0	0	0
0.587	0	1	1	2
0.511	0	0	0	0
0.421	0	1	0	1
0.4	0	0	1	1
0.3	0	1	0	1
0.294	0	1	1	2
0.21	1	0	0	1
0.129	0	1	1	2
0.06	1	0	0	1

Table 4.
Closeness of billboard, gates, or metal fences with respect to the differential of radiation density.

Real-normal differential	2-floor buildings	Buildings of 3 or more floors	Amount	Amount > 0
16.95	1	0	1	1
16.14	1	0	1	1
7.71	1	0	1	1
4.134	1	1	2	1
4.05	1	0	1	1
2.859	1	0	1	1
2.772	1	1	2	1
2.609	1	0	1	1
2.026	1	0	1	1
1.602	1	0	1	1
1.26	1	0	1	1
1.19	0	1	1	1
1.161	0	0	0	0
1.138	0	0	0	0
1.067	1	0	1	1
0.935	1	0	1	1
0.9	1	0	1	1
0.883	0	1	1	1
0.85	0	0	0	0
0.811	0	0	0	0
0.81	1	1	2	1
0.719	0	1	1	1
0.7	1	0	1	1
0.667	1	0	1	1
0.663	1	0	1	1
0.621	1	0	1	1
0.601	1	0	1	1
0.587	1	0	1	1
0.511	0	0	0	0
0.421	1	0	1	1
0.4	1	0	1	1
0.3	1	0	1	1
0.294	0	1	1	1
0.21	1	0	1	1
0.129	1	0	1	1
0.06	1	1	2	1
Total	27	8		31

Table 5.
Relationship between nearby buildings and the radiation level differential.

Real-normal differential	High-density electrical wiring	High-density parked vehicles	Site under plants	Metal ceilings nearby
16.95	1	1	1	0
16.14	0	0	1	1
7.71	1	1	1	0
4.134	0	1	0	0
4.05	0	0	1	1
2.859	1	1	1	0
2.772	0	0	0	0
2.609	0	1	0	1
2.026	0	0	0	0
1.602	0	0	0	0
1.26	1	0	0	0
1.19	1	1	0	1
1.161	0	0	0	0
1.138	0	0	0	0
1.067	0	1	0	0
0.935	0	0	0	0
0.9	0	1	0	0
0.883	0	1	0	1
0.85	0	0	0	1
0.811	0	0	0	0
0.81	0	1	1	0
0.719	0	1	0	1
0.7	1	0	0	1
0.667	0	0	0	0
0.663	0	1	0	1
0.621	1	1	0	0
0.601	0	0	0	0
0.587	0	0	0	0
0.511	0	0	0	1
0.421	0	1	0	0
0.4	0	0	1	0
0.3	1	0	0	0
0.294	1	0	0	0
0.21	1	0	1	0
0.129	1	0	0	0
0.06	1	1	0	0

Table 6.
Influence of other factors on the increase in the difference in radiation density.

High levels:

- 63% cars
- 63% plants
- 38% roofs

Low levels:

- 34% cars
- 10% plants
- 24% ceilings

The presence of cars parked in the vicinity, plants or trees on the measurement area, and to lesser extent metal roofs have a strong influence on the point value, such that in the values above the average of 2.12 uW/cm^2, the presence of these factors is verified. On the other hand, in low radiation values, there are no such conditions. Therefore, it can be concluded that vehicles and some types of plants contribute to the possibility of an increase in the level of radiation density.

It is also observed that at the highest levels there is the presence of two of these conditions.

8. Conclusions

There is no doubt that electromagnetic radiation has a number of variables whose study is constantly evolving, at the same time as technology evolves. New radiation patterns are incorporated to make the calculation more accurate and the behavior of electromagnetic waves more predictive.

In this work, it is demonstrated by field exploration in urban and suburban environments that there are points of high concentration of radiation, that these points have locations not related to the distance to the source, which are only points and not extensive areas with smaller radii than 4 meters, and that you can evaluate possibilities of existence of these points based on the surrounding environment, taking into account metallic surfaces at level and above ground level, constructions of more than one plant nearby, and to a lesser extent other factors, but in some cases, they are definitive in the location of what can be called hot spots of differential density of non-ionizing radiation.

Acknowledgements

The authors wish to express their gratitude to the Research Council of the Catholic University of Salta (UCASAL) for their support in the development of the research.

Conflict of interest

The authors declare that there is no potential conflict of interest related to the article.

Author details

Mario Marcelo Figueroa de la Cruz[1,2*] and Roberto Daniel Breslin[1]

1 Catholic University of Salta (UCASAL), Salta, Argentina

2 National Technological University, Tucuman, Argentina

*Address all correspondence to: mfiguero@gmail.com

References

[1] ADU4518R3. DXX-790-960/1710-2180-65/65-16.5i/18.5i-M/M-R. EasyRET Dual-Band Antenna with 2 Integrated RCUs. Electrical. Frequency range (MHz). Available from: https://www.huawei.com/ucmf/groups/public/documents/attachments/hw_316934.pdf [Accessed: 05-01-2019]

[2] Wireless Calculators. Available from: http://www.terabeam.com/support/calculations/index.php [Accessed: 05-01-2019]

[3] WNI Mexico Types of Antennas and Operation. Available from: https://www.wni.mx/index.php?option=com_content&view=article&id=62:antenassoporte&catid=31:general&Itemid=79 [Accessed: 05-01-2019]

[4] Reuse of the Mobile Telephone System. Basic Antennas. Available from: http://antenasupv.blogspot.com/2008/07/reutilizacin-del-sitema-de-telefonia.html [Accessed: 15-10-2018]

[5] Chapter 5 Propagation Models. Available from: http://catarina.udlap.mx/u_dl_a/tales/documentos/lem/trevino_c_jt/capitulo5.pdf [Accessed: 15-10-2018]

[6] National Communications Commission (CNC), National Communications Agency (ENACOM) Resolution N° 3690/2004

[7] Azpurua M, Teixeira K, Bolívar G, Aguilar R. Evaluation of exposure to radio frequency electromagnetic fields in urban environments using spatial analysis techniques based on geographical information systems. In: Proceedings of the IV International Event of Applied Electromagnetism CNEA 2011; Santiago de Cuba March 15-18, 2011

[8] Rios Solar J. Study of non-ionizing radiations for a base station Gsm 850 Mhz located in the Private University Antenor Orrego De Trujillo [thesis]. Trujillo: Perú Private University Antenor Orrego—UPAO; 2011

[9] Figueroa de la Cruz M, Breslin R, Narváez P. Measurements of non-ionizing radiations. In: Proceedings of the VI Working Meeting on Information Processing and Control; Salta Argentina; November 17 and 18, 2016

[10] Figueroa de la Cruz M, Narvaez P, Breslin R, Den Herder T. Analysis of measurements of non-ionizing radiation in the city of Salta from the UCASAL. No. of project 123/14 [thesis]. Salta Argentina Catholic University of Salta; 2016

[11] Definition—Definition and Etymology of Words. Available from: https://definiciona.com/inmision [Accessed: 27-10-2018]

[12] Oxford Dictionary. Available from: https://es.oxforddictionaries.com/definicion/aglutinacion [Accessed: 27-10-2018]

[13] Linear Technology—LTC5533 Schottky Peak Detector. Available from: https://www.analog.com/media/en/technical-documentation/data-sheets/5534fc.pdf [Accessed: 17-10-2018]

[14] Katrin K. Surface-enhanced Raman scattering. Physics Today. 2007. DOI: 10.1007/11663898

[15] Oldenburg SJ, Hale GD, Jackson JB, Halas NJ. Light scattering from dipole and quadrupole nanoshell antennas. Applied Physics Letters. 1999;**75**:1063. DOI: 10.1063/1.124597

[16] Martin M. Surface-enhanced spectroscopy. Reviews of Modern Physics. 1985;**57**:783. DOI: 10.1007/3-540-33567-6_1

[17] Rodriguez-Fortuño F, Marino G, Ginzburg P, O'Connor D, Martinez A, Gregory A. Near-field interference for the unidirectional excitation of electromagnetic guided modes. Science. 2013;**340**(6130):328-330. DOI: 10.1126/science.1233739

[18] RECOMMENDATION ITU-R P.526-11 Available from: https://www.itu.int/dms_pubrec/itu-r/rec/p/R-REC-P.526-11-200910-S!!PDF-S.pdf [Accessed: 27-10-2018]